journal

J. Am. Ceram. Soc., ■■ [■■] 1–10 (2011)
DOI: 10.1111/j.1551-2916.2011.04432.x

Large Plastic Deformation in High-Capacity Lithium-Ion Batteries Caused by Charge and Discharge

Kejie Zhao, Matt Pharr, Shengqiang Cai, Joost J. Vlassak, and Zhigang Suo†

School of Engineering and Applied Sciences, Kavli Institute for Bionano Science and Technology, Harvard University, Cambridge, Massachusetts 02138

Evidence has accumulated recently that a high-capacity electrode of a lithium-ion battery may not recover its initial shape after a cycle of charge and discharge. Such a plastic behavior is studied here by formulating a theory that couples large amounts of lithiation and deformation. The homogeneous lithiation and deformation in a small element of an electrode under stresses is analyzed within nonequilibrium thermodynamics, permitting a discussion of equilibrium with respect to some processes, but not others. The element is assumed to undergo plastic deformation when the stresses reach a yield condition. The theory is combined with a diffusion equation to analyze a spherical particle of an electrode being charged and discharged at a constant rate. When the charging rate is low, the distribution of lithium in the particle is nearly homogeneous, the stress in the particle is low, and no plastic deformation occurs. When the charging rate is high, the distribution of lithium in the particle is inhomogeneous, and the stress in the particle is high, possibly leading to fracture and cavitation.

I. Introduction

Lithium-ion batteries are being developed to achieve safe operation, high capacity, fast charging, and long life. Each electrode in a lithium-ion battery is a host of lithium.[1] Lithium diffuses into and out of the electrode when the battery is charged and discharged. If a particle of the electrode material is charged or discharged slowly and is unconstrained by other materials, the distribution of lithium in the particle is nearly homogeneous, and the particle expands or contracts freely, developing no stress. In practice, however, charge and discharge cause a field of stress in the particle when the distribution of lithium is inhomogeneous,[2–5] when the host contains different phases,[6] or when the host is constrained by other materials.[7] The stress may cause the electrode to fracture,[6–10] which may lead the capacity of the battery to fade.[11–14]

Lithiation-induced fracture not only occurs in current commercial lithium-ion batteries, but is also a bottleneck in developing future lithium-ion batteries.[15,16] For example, of all known materials for anodes, silicon offers the highest theoretical specific capacity—each silicon atom can host up to 4.4 lithium atoms. By comparison, in commercial anodes of graphite, every six carbon atoms can host up to one lithium atom. However, silicon is not used in anodes in commercial lithium-ion batteries, mainly because the capacity of silicon fades after a small number of cycles—a mode of failure often attributed to lithiation-induced fracture.

Recent experiments, however, have shown that the capacity can be maintained over many cycles for silicon anodes of small feature sizes, such as thin films,[17] nanowires,[18] and porous structures.[19] When silicon is fully lithiated, the volume of the material swells by $\sim 300\%$.[15] For anodes of small feature sizes, evidence has accumulated recently that this lithiation-induced strain can be accommodated by plastic deformation. For instance, cyclic lithiation causes 50-nm-thick silicon films to develop undulation without fracture.[17] Likewise, cyclic lithiation causes surfaces of silicon nanowires to roughen.[18] These studies suggest that lithiated silicon undergoes plastic deformation. Furthermore, during cyclic lithiation of an amorphous silicon thin film attached to a substrate, the measured relation between the stress in the film and the state of charge exhibits pronounced hysteresis.[20] This observation indicates that the lithiated silicon film deforms plastically when the stress exceeds a yield strength. At this writing, the atomistic mechanism of plastic flow of lithiated silicon is unclear, but is possibly due to a "lubricating effect" of lithium. Cyclic lithiation and delithiation can also cause silicon to grow cavities.[21]

This paper develops a theory of finite plastic deformation of electrodes caused by charge and discharge. Plastic deformation has not been considered in most existing theories of lithiation-induced deformation.[2–10] The works that do include plasticity have been limited to small deformation.[22,23] Here, we analyze the homogeneous lithiation and deformation in a small element of an electrode within nonequilibrium thermodynamics, stipulating equilibrium with respect to some processes, but not others. The element is assumed to undergo plastic deformation when the state of stress reaches a yield condition. We then combine large plastic deformation and diffusion to analyze the lithiation of a spherical particle of an electrode. When a small particle is charged and discharged slowly, the stress is small. When the particle is charged and discharged quickly, the stress is high, potentially leading to fracture or cavitation.

II. Nonequilibrium Thermodynamics of Coupled Lithiation and Deformation

Figure 1 illustrates an element of an electrode subject to a cycle of charge and discharge. The element is small in size, so that fields in the element are homogeneous. In the reference state (Fig. 1(a)), the element is a unit cube of a host material, free of lithium and under no stress. When the element is connected to a reservoir of lithium at chemical potential μ and is subject to stresses s_1, s_2, and s_3, as illustrated in Fig. 1(b), the element absorbs a number C of lithium atoms, becomes a block of sides λ_1, λ_2, and λ_3, and gains in free energy W.

By definition, s_1, s_2, and s_3 are nominal stresses—forces acting on the element in the current state divided by the areas of the element in the reference state. The true stresses, σ_1, σ_2, and σ_3, are forces per unit areas of the element in the current state. The true stresses relate to the nominal stresses by $\sigma_1 = s_1/(\lambda_2\lambda_3)$, $\sigma_2 = s_2/(\lambda_3\lambda_1)$, and $\sigma_3 = s_3/(\lambda_1\lambda_2)$.

Associated with small changes in the stretches, $\delta\lambda_1$, $\delta\lambda_2$, and $\delta\lambda_3$, the forces do work $s_1\delta\lambda_1 + s_2\delta\lambda_2 + s_3\delta\lambda_3$. Associated with small change in the number of lithium atoms, δC, the chemical potential does work $\mu\delta C$. Thermodynamics dictates that the

R. McMeeking—contributing editor

Manuscript No. 28712. Received October 2, 2010; approved January 4, 2011.
This work is supported by the National Science Foundation through a grant on Lithium-ion Batteries (CMMI-1031161).
†Author to whom correspondence should be addressed. e-mail: suo@seas.harvard.edu

combined work should be no less than the change in the free energy:

$$s_1\delta\lambda_1 + s_2\delta\lambda_2 + s_3\delta\lambda_3 + \mu\delta C \geq \delta W \quad (1)$$

The work done minus the change in the free energy is the dissipation. The inequality (1) means that the dissipation is non-negative with respect to all processes. The object of this section is to examine the large amounts of lithiation and deformation by constructing a theory consistent with the thermodynamic inequality (1).

As illustrated in Fig. 1(b), when the unit cube of the host is lithiated under stresses, the deformation is anisotropic: the unit cube will change both its shape and volume. For example, a thin film of an electrode constrained on a stiff substrate, upon absorbing lithium, deforms in the direction normal to the film, but does not deform in the directions in the plane of the film.

The material deforms by mechanisms of two types: inelastic and elastic. Inelastic deformation involves mixing and rearranging atoms. Elastic deformation involves small changes of the relative positions of atoms, retaining the identity of neighboring atoms as well as the concentration of lithium. When the stresses are removed and the reservoir of lithium is disconnected, the material element will retain part of the anisotropic deformation (Fig. 1(c)). The phenomenon is reminiscent of plasticity of a metal. The remaining deformation is characterized by three stretches λ_1^i, λ_2^i, and λ_3^i, which we call inelastic stretches. The part of deformation that disappears upon the removal of the stresses is characterized by three stretches λ_1^e, λ_2^e, and λ_3^e, which we call elastic stretches. The total stretches are taken to be the products of the two types of the stretches

$$\lambda_1 = \lambda_1^e\lambda_1^i, \quad \lambda_2 = \lambda_2^e\lambda_2^i, \quad \lambda_3 = \lambda_3^e\lambda_3^i \quad (2)$$

Similar multiplicative decomposition is commonly used to describe elastic–plastic deformation of metals[24] and polymers,[25] as well as growth of tissues.[26]

We characterize the state of the material element by a total of seven independent variables: λ_1^e, λ_2^e, λ_3^e, λ_1^i, λ_2^i, λ_3^i and C.

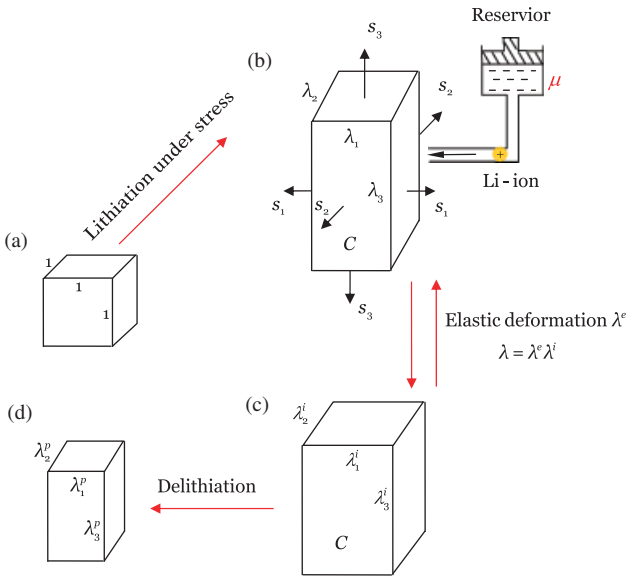

Fig. 1. After a cycle of lithiation and delithiation, an electrode material may not recover its initial shape. (a) In the reference state, an element of an electrode material is a lithium-free and stress-free unit cube. (b) Subject to forces and connected to a reservoir of lithium, the material element absorbs lithium, and undergoes anisotropic deformation. (c) When the stresses are removed and the reservoir of lithium is disconnected, the material element unloads elastically, and the remaining inelastic deformation is anisotropic. (d) After the material element desorbs lithium under no stress, the lithium-free host becomes a rectangular block.

Plasticity of a metal and inelasticity of an electrode differ in a significant aspect. While plastic deformation of a metal changes shape but conserves volume, inelastic deformation of an electrode changes both volume and shape. We decompose the inelastic stretches by writing

$$\lambda_1^i = \Lambda^{1/3}\lambda_1^p, \quad \lambda_2^i = \Lambda^{1/3}\lambda_2^p, \quad \lambda_3^i = \Lambda^{1/3}\lambda_3^p \quad (3)$$

Here, Λ is the volume of the material element after the removal of the stresses, namely,

$$\lambda_1^i\lambda_2^i\lambda_3^i = \Lambda \quad (4)$$

Inelastic shape change of the material element is described by λ_1^p, λ_2^p, and λ_3^p (Fig. 1(d)). By the definition of (3) and (4), the plastic stretches do not change volume, namely,

$$\lambda_1^p\lambda_2^p\lambda_3^p = 1 \quad (5)$$

We will call λ_1^p, λ_2^p, and λ_3^p the plastic stretches. In our terminology, inelastic deformation includes the changes in both volume and shape, while plastic deformation involves only the change in shape.

A combination of (2) and (3) gives $\lambda_1 = \lambda_1^e\lambda_1^p\Lambda^{1/3}$. Taking the logarithm of both sides of this equation, we write $\log\lambda_1 = \log\lambda_1^e + \log\lambda_1^p + \log\Lambda^{1/3}$. The quantity $\log\lambda_1$ is the natural strain, $\log\lambda_1^e$ the elastic part of the natural strain, and $\log\lambda_1^p$ the plastic part of the natural strain.

Most existing theories of lithiation-induced deformation do not consider plasticity. In effect, these theories assume that, after a cycle of lithiation and delithiation, the material element recovers its initial shape. Such an assumption disagrees with experimental observations of lithiation of large-capacity hosts, such as silicon, as discussed in the Introduction and in several recent papers.[22,23,27] This paper will allow plasticity, and will describe rules to calculate large plastic deformation.

The state of the element can be characterized by an alternative list of seven independent variables: λ_1^e, λ_2^e, λ_3^e, λ_1^p, λ_2^p, Λ, and C. To progress further, we make the following simplifying assumptions. The inelastic expansion of the volume is taken to be entirely due to the absorption of lithium, and is a function of the concentration of lithium:

$$\Lambda = \Lambda(C) \quad (6)$$

This function is taken to be characteristic of the material, and is independent of the elastic and plastic stretches. Equation (6) eliminates Λ from the list of independent variables, so that the state of the material element is characterized by six independent variables: λ_1^e, λ_2^e, λ_3^e, λ_1^p, λ_2^p, and C.

Following the theory of plasticity, we assume that the free energy of the material element is unaffected by the plastic stretches. Thus, the free energy is a function of four variables:

$$W = W(\lambda_1^e, \lambda_2^e, \lambda_3^e, C) \quad (7)$$

This assumption is understood as follows. The plastic stretches characterize inelastic shape change, involving rearranging atoms without changing the concentration of lithium. This rearrangement of atoms may dissipate energy, but does not alter the amount of free energy stored in the host materials. The situation is reminiscent of shear flow of a liquid of small molecules—the free energy is stored in molecular bonds, independent of the amount of flow. For a work-hardening metal, however, plastic strain will change the free energy stored in the material, for example, by creating more dislocations. Thus, assuming (7) amounts to a stipulation that plastic strains do not create such microstructural changes in lithiated electrodes.

Rewriting the inequality (1) in terms of the changes in the six independent variables, λ_1^e, λ_2^e, λ_3^e, λ_1^p, λ_2^p, and C, we obtain that

$$\left(\sigma_1\lambda_1\lambda_2\lambda_3 - \frac{\partial W}{\partial \log \lambda_1^e}\right)\delta \log \lambda_1^e + \left(\sigma_2\lambda_1\lambda_2\lambda_3 - \frac{\partial W}{\partial \log \lambda_2^e}\right) \times \delta \log \lambda_2^e + \left(\sigma_3\lambda_1\lambda_2\lambda_3 - \frac{\partial W}{\partial \log \lambda_3^e}\right)\delta \log \lambda_3^e + \left(\mu - \frac{\partial W}{\partial C} + \Omega\sigma_m\right)\delta C + \lambda_1\lambda_2\lambda_3\left[(\sigma_1 - \sigma_3)\delta \log \lambda_1^p + (\sigma_2 - \sigma_3)\delta \log \lambda_2^p\right] \geq 0 \tag{8}$$

where $\sigma_m = (\sigma_1+\sigma_2+\sigma_3)/3$ is the mean stress, and $\Omega = \lambda_1^e\lambda_2^e\lambda_3^e d\Lambda(C)/dC$ is the volume per lithium atom in the host.

Each of the six independent variables represents a process to evolve the material. The processes take place at different rates. We will adopt a commonly used simplifying approach. Say that we are interested in a particular time scale. Processes taking place faster than this time scale are assumed to be instantaneous. Processes taking place slower than this time scale are assumed to never occur. In the present problem, the particular time scale of interest is the time needed for a particle of an electrode material of a finite size to absorb a large amount of lithium. This time is taken to be set by the diffusion time scale.

Elastic relaxation is typically much faster than diffusion. We assume that the material element is in equilibrium with respect to the elastic stretches, so that in (8) the coefficients associated with $\delta\lambda_1^e$, $\delta\lambda_2^e$, and $\delta\lambda_3^e$ vanish:

$$\sigma_1 = \frac{\partial W}{\lambda_1\lambda_2\lambda_3\partial \log \lambda_1^e},\ \sigma_2 = \frac{\partial W}{\lambda_1\lambda_2\lambda_3\partial \log \lambda_2^e},\ \sigma_3 = \frac{\partial W}{\lambda_1\lambda_2\lambda_3\partial \log \lambda_3^e} \tag{9}$$

We further assume that the material element is in equilibrium with respect to the concentration of lithium, so that in (8) the coefficient of δC vanishes:

$$\mu = \frac{\partial W(\lambda_1^e, \lambda_2^e, \lambda_3^e, C)}{\partial C} - \Omega\sigma_m \tag{10}$$

The free energy is adopted in the following form:

$$W = W_0(C) + \Lambda G\left[(\log \lambda_1^e)^2 + (\log \lambda_2^e)^2 + (\log \lambda_3^e)^2 + \frac{\nu}{1-2\nu}(\log \lambda_1^e\lambda_2^e\lambda_3^e)^2\right] \tag{11}$$

where G is the shear modulus, and ν Poisson's ratio. Equation (11) can be interpreted as the Taylor expansion in terms of elastic strains. We have assumed that the elastic strains are small, and only retain terms up to those that are quadratic in strains. We have neglected any dependence of elastic moduli on the concentration of lithium. A combination of (9) into (11) shows that the stresses relate to the elastic strains as

$$\sigma_1 = 2G\left(\log \lambda_1^e + \frac{\nu}{1-2\nu}\log \lambda_1^e\lambda_2^e\lambda_3^e\right)$$
$$\sigma_2 = 2G\left(\log \lambda_2^e + \frac{\nu}{1-2\nu}\log \lambda_1^e\lambda_2^e\lambda_3^e\right)$$
$$\sigma_3 = 2G\left(\log \lambda_3^e + \frac{\nu}{1-2\nu}\log \lambda_1^e\lambda_2^e\lambda_3^e\right) \tag{12}$$

A combination (10) and (11) expresses the chemical potential of lithium as

$$\mu = \frac{dW_0(C)}{dC} - \Omega\sigma_m \tag{13}$$

In writing (12) and (13), we have neglected the terms quadratic in the elastic strains.

The material element, however, may not be in equilibrium with respect to plastic stretches. Consequently, the inequality (8) is reduced to

$$(\sigma_1 - \sigma_3)\delta \log \lambda_1^p + (\sigma_2 - \sigma_3)\delta \log \lambda_2^p \geq 0 \tag{14}$$

This thermodynamic inequality may be satisfied by many kinetic models—creep models that relate the rate of plastic strains to stresses. For simplicity, here we adopt a particular type of kinetic model: the model of time-independent plasticity.[28] A material is characterized by a yield strength. When the stress is below the yield strength, the rate of the plastic strain is taken to be so low that no additional plastic strain occurs. When the stress reaches the yield strength, the rate of plastic strain is taken to be so high that plastic strain increases instantaneously.

To calculate plastic deformation, we adopt the J_2 flow theory.[28] Recall that the plastic stretches preserve the volume, $\lambda_1^p\lambda_2^p\lambda_3^p = 1$. Consequently, (14) may be written in a form symmetric with respect to the three directions:

$$(\sigma_1 - \sigma_m)\delta \log \lambda_1^p + (\sigma_2 - \sigma_m)\delta \log \lambda_2^p + (\sigma_3 - \sigma_m)\delta \log \lambda_3^p \geq 0 \tag{15}$$

The J_2 flow theory is prescribed as

$$\delta \log \lambda_1^p = \alpha(\sigma_1 - \sigma_m),$$
$$\delta \log \lambda_2^p = \alpha(\sigma_2 - \sigma_m),$$
$$\delta \log \lambda_3^p = \alpha(\sigma_3 - \sigma_m) \tag{16}$$

where α is a nonnegative scalar. This flow theory is symmetric with respect to the three directions, satisfies $\lambda_1^p\lambda_2^p\lambda_3^p = 1$, and is consistent with the thermodynamic inequality (15). In numerical calculations performed later, we will assume that the material is perfectly plastic. Let σ_Y be the yield strength measured when the material element is subject to uniaxial stressing. The yield strength is taken to be a function of concentration alone, $\sigma_Y(C)$. When the material element is under multiaxial stressing, the equivalent stress is defined by

$$\sigma_e = \sqrt{\frac{3}{2}\left[(\sigma_1 - \sigma_m)^2 + (\sigma_2 - \sigma_m)^2 + (\sigma_3 - \sigma_m)^2\right]} \tag{17}$$

The material element yields under the von Mises condition: $\sigma_e = \sigma_Y(C)$. The value of α is specified by the following rules

$$\begin{cases} \alpha = 0, & \sigma_e < \sigma_Y \\ \alpha = 0, & \sigma_e = \sigma_Y, \quad \delta\sigma_e < \delta\sigma_Y \\ \alpha > 0, & \sigma_e = \sigma_Y, \quad \delta\sigma_e = \delta\sigma_Y \end{cases} \tag{18}$$

III. A Spherical Particle of an Electrode

We now apply the theory to a spherical particle of an electrode material (Fig. 2). We have previously solved this problem using a theory of small plastic deformation.[22] Here we will allow large deformation. We model such an inelastic host of lithium by considering coupled lithium diffusion and large elastic–plastic deformation. In the following paragraphs, we specify the kinematics of large deformation, the kinetics of lithium diffusion, the flow rule of plasticity, and the thermodynamics of lithiation. The results of an amorphous silicon particle during charge and discharge are shown in Section IV. The detailed numerical procedure is included in Appendix A.

Before absorbing any lithium, the particle is of radius A, and is stress-free. This lithium-free particle is taken to be the reference configuration. At time t, the particle absorbs some lithium,

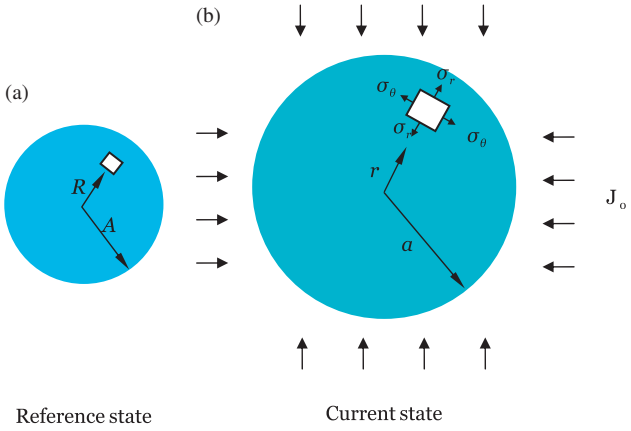

Fig. 2. (a) In the reference state, a spherical particle of an electrode is lithium-free and stress-free. (b) In the current sate, the particle is partially lithiated, and develops a field of stress.

the distribution of which may be inhomogeneous in the radial direction, but retains spherical symmetry. The inhomogeneous distribution of lithium induces in the particle a field of stress, and the particle swells to a radius a.

The kinematics of the large deformation is specified as follows. The spherical particle consists of a field of material elements. A material element a distance R from the center in the reference configuration moves, at time t, to a place a distance r from the center. The function $r(R, t)$ specifies the deformation of the particle. In representing a field, we may choose either r or R as an independent variable. One variable can be changed to the other by using the function $r(R, t)$. We will indicate our choice in each field explicitly when the distinction is important. The radial stretch is

$$\lambda_r = \frac{\partial r(R,t)}{\partial R} \tag{19}$$

The hoop stretch is

$$\lambda_\theta = \frac{r}{R} \tag{20}$$

The kinematics of lithium is specified as follows. Let C be the nominal concentration of lithium (i.e., the number of lithium atoms per unit volume of pure silicon in the reference state). The distribution of lithium in the particle is specified by the function $C(R, t)$. Because of the spherical symmetry, lithium diffuses in the radial direction. Let J be the nominal flux of lithium (i.e., the number of lithium atoms per unit reference area per unit time). The nominal flux is also a time-dependent field, $J(R, t)$. Conservation of the number of lithium atoms requires that

$$\frac{\partial C(R,t)}{\partial t} + \frac{\partial (R^2 J(R,t))}{R^2 \partial R} = 0 \tag{21}$$

Later we will also invoke the true concentration c (i.e., the number of lithium atoms per unit volume in the current configuration), and the true flux j (i.e., the number of lithium atoms per current area per time). These true quantities relate to their nominal counterparts by $J = j\lambda_\theta^2$ and $C = c\lambda_r\lambda_\theta^2$.

Write the radial stretch λ_r and the hoop stretch λ_θ in the form

$$\lambda_r = \lambda_r^e \lambda_r^p \Lambda^{1/3}, \ \lambda_\theta = \lambda_\theta^e \lambda_\theta^p \Lambda^{1/3} \tag{22}$$

We will mainly consider high-capacity hosts that undergo large deformation by lithiation, and will neglect the volumetric change due to elasticity, setting $\lambda_r^e(\lambda_\theta^e)^2 = 1$. Consistent with this assumption, we set Poison's ratio $\nu = 1/2$, and set Young's modulus $E = 3G$. Recall that by definition the plastic stretches preserve volume, $\lambda_r^p(\lambda_\theta^p)^2 = 1$.

In the spherical particle, each material element is subject to a state of triaxial stresses, $(\sigma_r, \sigma_\theta, \sigma_\theta)$, where σ_r is the radial stress, and σ_θ the hoop stress. The state of elastic–plastic deformation is taken to be unaffected when a hydrostatic stress is superimposed on the element. In particular, as illustrated in Fig. 3(a), superimposing a hydrostatic stress $(-\sigma_\theta, -\sigma_\theta, -\sigma_\theta)$ to the state of triaxial stresses $(\sigma_r, \sigma_\theta, \sigma_\theta)$ results in a state of uniaxial stress $(\sigma_r - \sigma_\theta, 0, 0)$. The state of elastic–plastic deformation of the element subject to the triaxial stresses is the same as the state of plastic deformation of the element subject to a uniaxial stress $\sigma_r - \sigma_\theta$. We represent the uniaxial stress–stretch relation by the elastic and perfectly plastic model. Figure 3(b) sketches this stress–strain relation in terms of the stress $\sigma_r - \sigma_\theta$ and the elastic–plastic part of the true strain, $\log(\lambda_r^e \lambda_r^p) = \log(\lambda_r \Lambda^{-1/3})$. The yield strength in the state of uniaxial stress, σ_Y, is taken to be a constant independent of the plastic strain and concentration of lithium.

In the spherical particle the stresses are inhomogeneous, represented by functions $\sigma_r(R, t)$ and $\sigma_\theta(R, t)$. The balance of forces acting on a material element requires that

$$\frac{\partial \sigma_r(R,t)}{\lambda_r \partial R} + 2\frac{\sigma_r - \sigma_\theta}{\lambda_\theta R} = 0 \tag{23}$$

We specify a material model of transport as follows. We assume that each material element is in a state of local equilibrium with respect to the reaction between lithium atoms and host atoms, so that we can speak of the chemical potential of lithium in the material element. We further assume that the chemical potential of lithium in the material element takes the form:

$$\mu = \mu^0 + kT\log(\gamma c) - \Omega\sigma_m \tag{24}$$

where μ^0 is a reference value, γ the activity coefficient, and c the true concentration of lithium.

If the distribution of lithium in the particle is inhomogeneous, the chemical potential of lithium is a time-dependent field, $\mu(r, t)$, and the particle is not in diffusive equilibrium. The gradient of the chemical potential drives the flux of lithium. We adopt a linear kinetic model:

$$j = -\frac{cD}{kT}\frac{\partial \mu(r,t)}{\partial r} \tag{25}$$

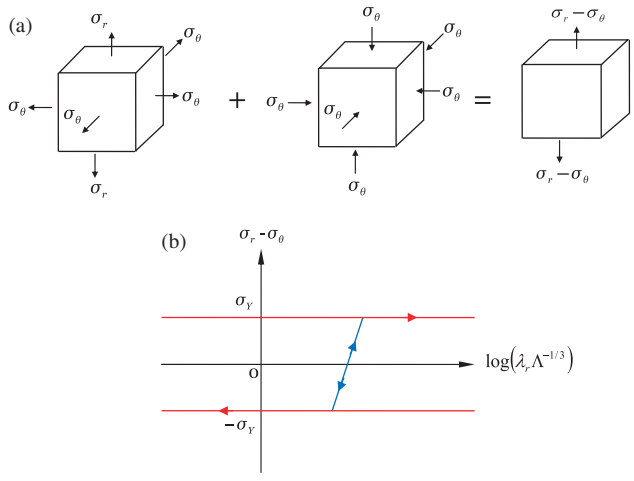

Fig. 3. (a) The state of elastic–plastic deformation of the element subject to the triaxial stresses $(\sigma_r, \sigma_\theta, \sigma_\theta)$ is the same as that of the element subject to a uniaxial stress $(\sigma_r - \sigma_\theta)$. (b) The uniaxial stress–strain relation in terms of the stress $(\sigma_r - \sigma_\theta)$ and the true elastic–plastic strain log $(\lambda_r \Lambda^{-1/3})$.

This relation has been written in a conventional form, in terms of the true flux j and the true concentration c. Note that kT is the temperature in dimensions of energy, and that (25) may be regarded as a phenomenological definition of the diffusivity D. Recall that the flux relates to the drift velocity of lithium in the host by $j = cv_{\text{drift}}$. Thus, D/kT is the mobility of lithium in the host. The diffusivity may depend on concentration and stress.

The particle is subject to the following boundary conditions. Because of the symmetry, $r(0, t) = 0$ and $J(0, t) = 0$. On the surface of the particle, the radial stress vanishes at all time, $\sigma_r(A, t) = 0$. The particle is charged and discharged by prescribing on the surface of the particle a constant flux J_0, namely, $J(A, t) = \pm J_0$. The signs differ for charge and discharge.

IV. Numerical Results and Discussions

We solve the initial-boundary value problem numerically, as described in Appendix A. This section describes the numerical results, and discusses their implications. For simplicity, we set $\gamma = 1$ and assume that Ω, E, σ_Y, and D are constant. The initial-boundary value problem has three dimensionless parameters: $\Omega E/kT$, σ_Y/E, and $J_0 A\Omega/D$. For lithium in amorphous silicon, representative values are $\Omega = 1.36 \times 10^{-29}$ m^3, $E = 80$ GPa, $\sigma_Y = 1.75$ GPa,[20] and $D = 10^{-16}$ m^2/s,[29] giving $\Omega E/kT = 263$ and $\sigma_Y/E = 0.022$. The parameter $J_0 A\Omega/D$ is a dimensionless measure of the charging rate, and may be interpreted as follows. Let $C_{\max}$ be the maximum theoretical concentration of lithium. When the spherical particle of radius A is charged by a constant flux J_0, the nominal time τ needed to charge the particle to the theoretical maximum concentration is given by $4\pi A^2 J_0 \tau = (4\pi A^3/3) C_{\max}$. For silicon, the volume of fully lithiated state swells by about 300%, so that $\Omega C_{\max} \approx 3$. For a particle of radius $A = 1$ μm, $\tau = 1$ h corresponds to $J_0 A\Omega/D = 2.8$. In the following description, we use τ to represent the charge rate; for example, $\tau = 0.5$ h means that it needs 0.5 h to charge silicon to reach the theoretical maximum lithium concentration. Smaller values of τ represent a faster charge process. We normalize time as Dt/A^2. For a particle of radius $A = 1$ μm, the diffusion time scale is $A^2/D = 10^4$ s.

Figure 4 shows the evolution of the fields in the spherical particle charged at the rate of $\tau = 1$ h. The simulation is initiated when the particle is lithium-free, and is terminated when the concentration at the surface of the particle reaches the full capacity, $\Omega C_{\max} = 3$, and the interior of the particle is still much below the full capacity (Fig. 4(a)). At all time, $r(R, t) > R$, indicating all material elements in the particle move away from the center of the particle (Fig. 4(b)). The ratio λ_r/λ_θ measures the anisotropy of the deformation (Fig. 4(c)). The deformation is highly anisotropic near the surface of the particle, but is isotropic at the center of the particle. Plastic deformation occurs near the surface of the particle, but is absent at the center of the particle (Fig. 4(d)). The chemical potential of lithium in the particle is inhomogeneous, driving lithium to diffuse from the surface of the particle toward the center (Fig. 4(e)).

Figures 4(f)–(h) show the distributions of the radial, hoop and equivalent stresses. The traction-free boundary condition requires that the radial stress at the surface of the particle to vanish at all times. Because the distribution of lithium in the particle is inhomogeneous, the particle expands more near the surface than at the center, resulting in tensile radial stresses inside the particle. The hoop stress is compressive near the surface, and tensile near the center. For the spherical particle, the equivalent stress is $\sigma_e = |\sigma_\theta - \sigma_r|$, which is bounded in the interval $0 \le \sigma_e \le \sigma_Y$. By symmetry, the center of the sphere is under equal-triaxial tensile stresses. Because of the triaxial constraint at the center, the radial stress and hoop stress can exceed the yield strength.

The high level of tensile stresses at the center of the sphere may generate cavities. An experimentally measured value of the yield strength is $\sigma_Y = 1.75$ GPa.[20] Our calculation indicates that the stress at the center of the particle can be several times the yield strength. Let ρ be the radius of a flaw and γ_{surface} be the surface energy. For the flaw to expand, the stress needs to overcome the effect of the Laplace pressure, $2\gamma_{\text{surface}}/\rho$. Taking $\gamma_{\text{surface}} = 1$ J/m^2, we estimate that the critical radius $\rho = 1$ nm when the stress at the center of the particle is 2 GPa. Lithiation-induced cavitation has been observed in a recent experiment.[21]

To illustrate effects of yielding, Fig. 5 compares the two cases: $\sigma_Y = 1.75$ GPa and $\sigma_Y = \infty$ (no yielding). The fields are plotted at time $Dt/A^2 = 0.048$. As expected, yielding allows the particle to accommodate lithiation by greater anisotropic deformation, Fig. 5(b). Yielding also significantly reduces the magnitudes of the stresses, Figs. 5(c) and (d). This observation implies that fracture and cavitation may be avoided for electrodes with low yield strength.

As shown by (24), the chemical potential of lithium depends on the mean stress. This effect of stress on chemical potential has been neglected in some of the previous models. The representative values $\Omega = 1.36 \times 10^{-29}$ m^3 and $\sigma_Y = 1.75$ GPa give an estimate $\Omega\sigma_Y = 0.15$ eV, which is a value significant compared with the value of the term involving concentration in the expression of the chemical potential. Figure 6 compares results calculated by including or neglecting the term $\Omega\sigma_m$ in the expression of the chemical potential (24). The mean stress σ_m is compressive near the surface of the particle and tensile at the center. Consequently, the gradient of the mean stress also motivates lithium to migrate toward the center. Here we show the fields at the time when the surface of the particle attains the full capacity. The case with the mean stress included in the expression of the chemical potential absorbs more lithium at the center, Fig. 6(a). The stress gradient also decreases the chemical potential of lithium in the particle, Fig. 6(b). The contribution of the stress to the chemical potential helps to homogenize lithium distribution, and consequently reduces the stress.

Figure 7 compares the fields for three charging rates, $\tau = 0.5$ h, $\tau = 1$ h and $\tau = 2$ h. Each simulation is terminated when the surface of the particle attains the full capacity. The stress level is determined by the total amount of lithium inserted into the particle and the degree of inhomogeneity in the distribution of this amount of lithium. At a high charging rate, $\tau = 0.5$ h, the distribution of lithium is highly inhomogeneous, as in Fig. 7(a). However, the surface of the particle reaches its full capacity very rapidly. At this time, not much lithium has been inserted into the particle, so the stresses are fairly low and the deformation is anisotropic only near the surface of the particle. At such a fast charging rate, the particle will not store much lithium. At an intermediate charging rate, $\tau = 1$ h, lithium has some time to diffuse toward the center of the particle, but not enough time to fully homogenize the distribution of lithium. Consequently, relatively large stresses develop and the deformation is quite anisotropic. At a yet slower charging rate, $\tau = 2$ h, there is enough time for diffusion to nearly homogenize the distribution of lithium. At this slow charging rate, the particle is effective as an electrode in that it can store a large amount of lithium before the surface of the particle reaches the full capacity. This homogenization leads to relatively low stresses and nearly isotropic deformation.

Figure 8 shows the time evolution of the stress at the center of the particle for three charging rates. For a fast charging case ($\tau = 0.5$ h), the stress builds up until the outer surface reaches its full capacity. At an intermediate charging rate ($\tau = 1$ h), the stress builds up until it is large enough to significantly contribute to the chemical potential. At this point, both the stress gradient and concentration gradients tend to homogenize the concentration of lithium, and the stress decreases. However, the charging rate is still fairly fast relative to the time for diffusion. Thus, the concentration of lithium cannot be fully homogenized and the stress cannot be fully relaxed before the surface of the particle reaches the full capacity. By contrast, for the case of $\tau = 2$ h, the charging rate is slow enough for diffusion to homogenize the distribution of lithium before the surface of the particle reaches the full capacity, as shown in Fig. 7(a). As the distribution of

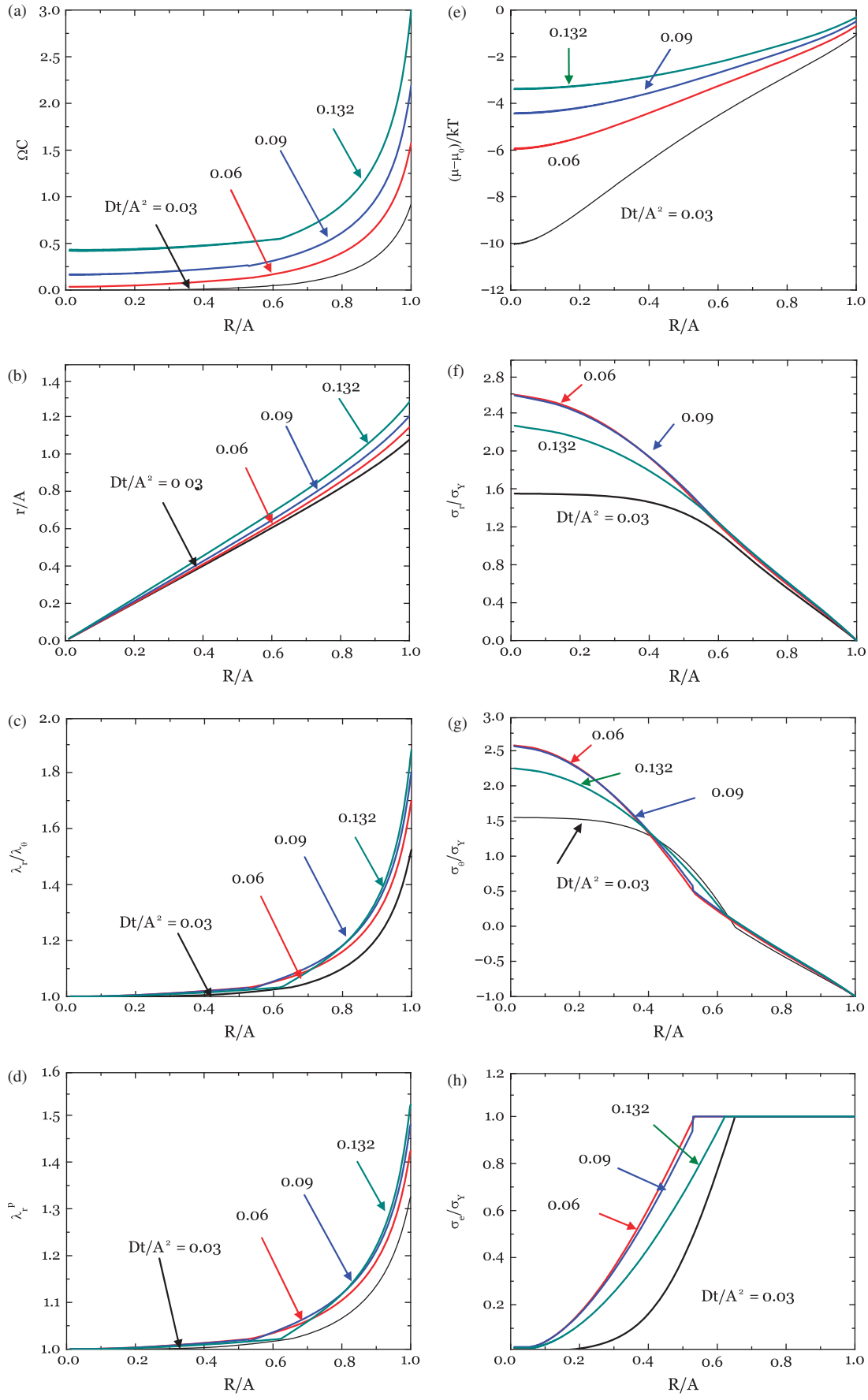

Fig. 4. As a spherical particle is being charged at the rate of $\tau = 1$ h, various fields evolve: (a) concentration of lithium, (b) deformation field, (c) ratio of the radial stretch to the hoop stretch, (d) plastic stretch in the radial direction, (e) chemical potential of lithium, (f) radial stress, (g) hoop stress, and (h) equivalent stress.

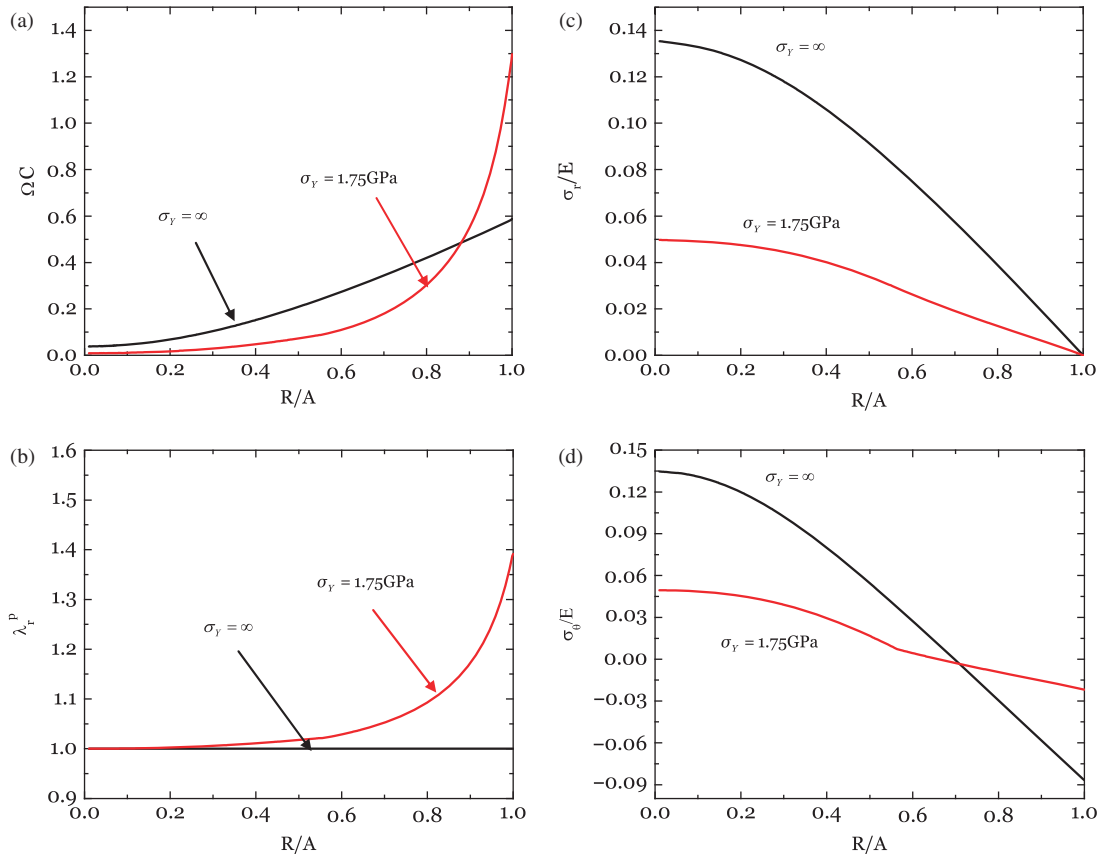

Fig. 5. The effect of plastic yield on various fields: (a) concentration of lithium, (b) plastic stretch in radial direction, (c) radial stress, and (d) hoop stress. The charging rate is $\tau = 1$ h, and the fields are given at time $Dt/A^2 = 0.048$.

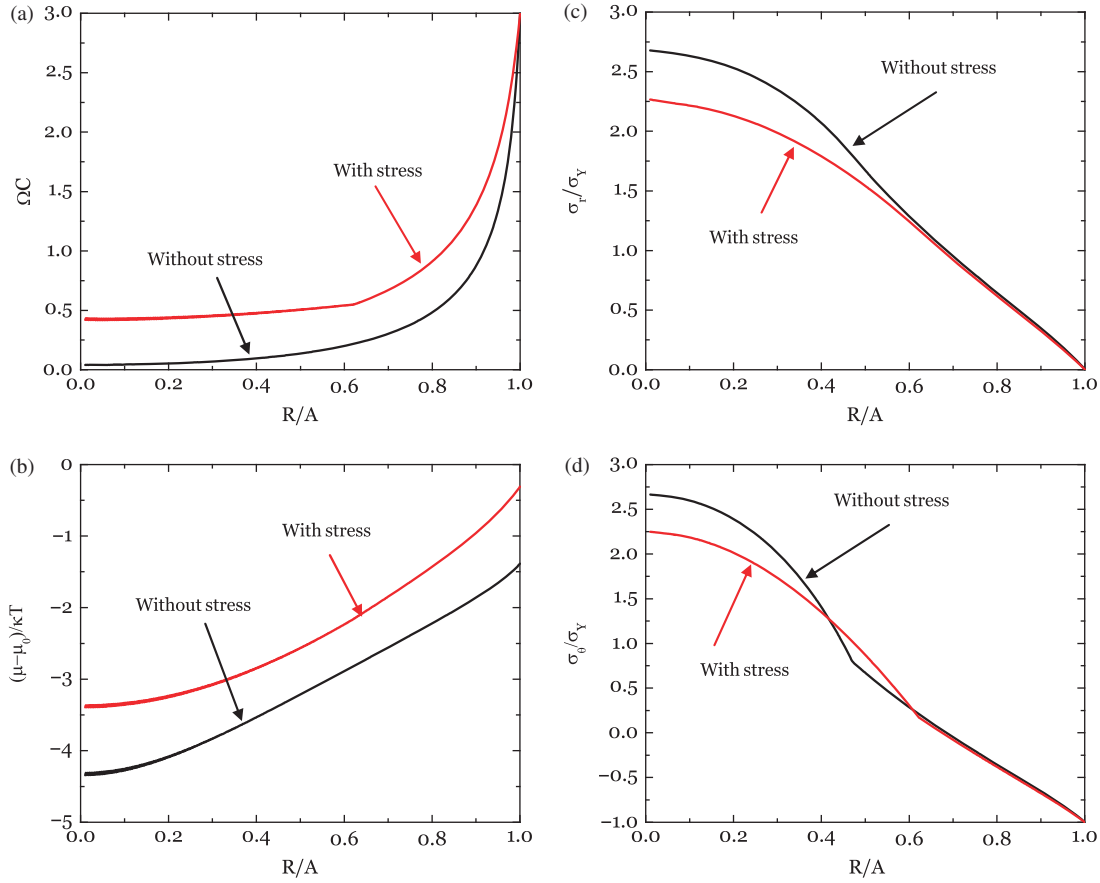

Fig. 6. Fields calculated with or without including the mean stress in the expression of the chemical potential of lithium are compared: (a) concentration of lithium, (b) chemical potential of lithium, (c) radial stress, and (d) hoop stress. The charging rate is $\tau = 1$ h, and both fields are given at the end of charge time, i.e., $Dt/A^2 = 0.132$ with stress calculation, $Dt/A^2 = 0.009$ without stress calculation.

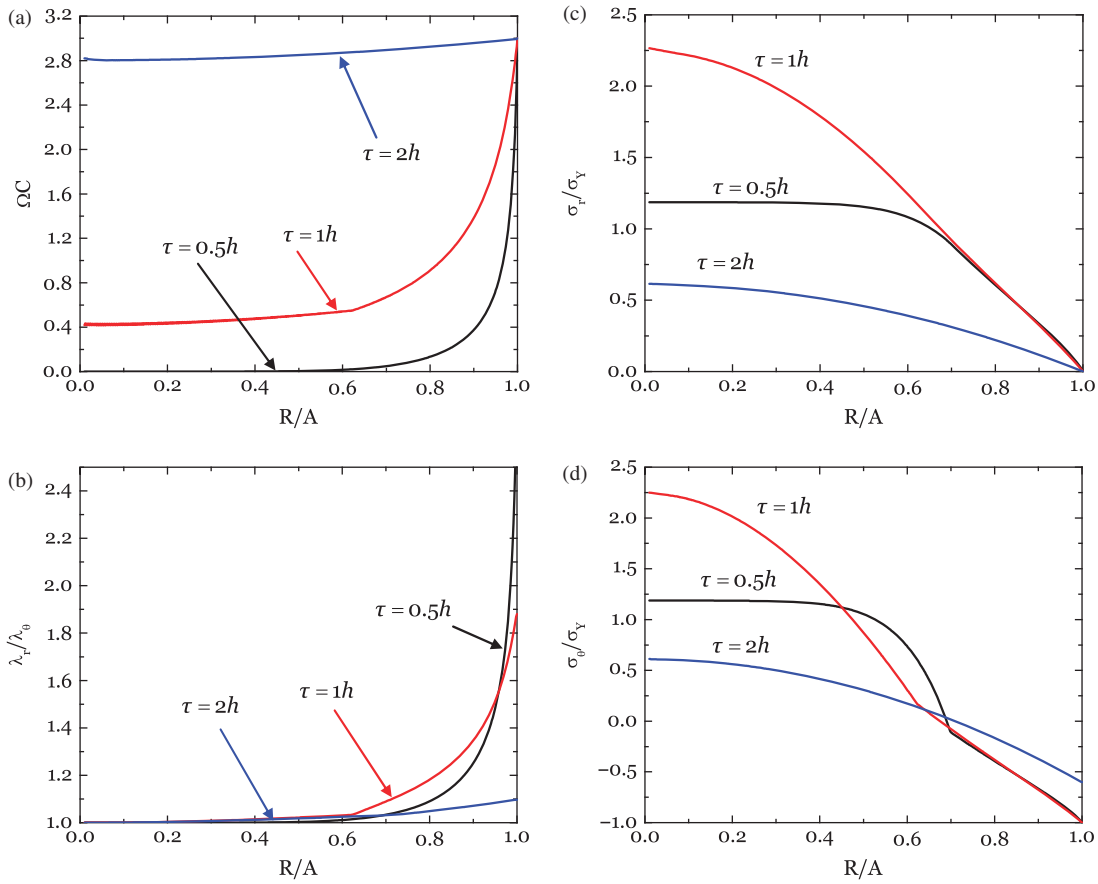

Fig. 7. The effect of the charging rate on various fields: (a) concentration of lithium, (b) ratio of radial stretch to hoop stretch, (c) radial stress, and (d) hoop stress.

lithium is homogenized, the stress is relaxed, as shown in Fig. 8. The effect of the charging rate on the triaxial tension at the center of the particle may be used to guide future experiments to study cavitation.

Figure 9 shows the time evolution of the lithium concentration and the stress fields as lithium desorbs from the spherical particle. The simulation begins when the particle is at full capacity of lithium and is stress-free, and is terminated when the concentration of lithium vanishes near the surface of the particle. As lithium desorbs, the concentration near the surface becomes lower than it is near the center of the particle, Fig. 9(a). This inhomogeneity causes the particle to contract more near the surface than at the center. Consequently, a compressive radial stress develops, Fig. 9(b). The hoop stress at the surface becomes tensile with magnitude σ_Y, Fig. 9(c). This tensile stress may result in the propagation of surface flaws. Because the tensile stress is limited by the yield strength, fracture may be averted when the yield strength is low.

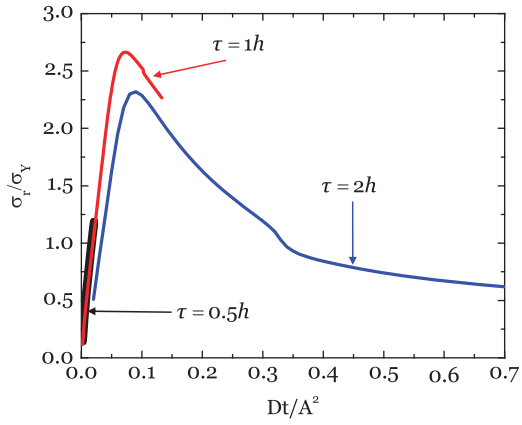

Fig. 8. The radial stress at the center of the sphere as a function of time at various charge rates.

V. Conclusions

This paper formulates a theory that couples lithiation and large elastic–plastic deformation. The homogeneous lithiation and deformation in a small material element is analyzed using non-equilibrium thermodynamics. The material is assumed to undergo plastic deformation when the state of stress reaches the yield condition. A spherical particle subject to a constant rate of charge and discharge is analyzed by coupling diffusion and large plastic deformation. The effect of plastic yielding, stress on the chemical potential of lithium, and charging rates are studied. When the charging rate is low, the distribution of lithium in the particle is nearly homogeneous, and the stress is low. When the charging rate is high, the stress at the center of the particle can substantially exceed the yield strength. The developed stress gradient also greatly influences the diffusion of lithium, tending to homogenize the distribution of lithium in the particle. Plastic yielding can markedly reduce the magnitude of stress.

Appendix A: Notes on Numerical Procedure

We rewrite the governing equations in the form used in our numerical simulation. It has been assumed that neither elastic nor plastic deformation causes any volumetric change. It has been also assumed that Ω is a constant. Consequently, the volumetric change of a material element is

$$\lambda_r\lambda_\theta^2 = 1 + \Omega C \qquad \text{(A-1)}$$

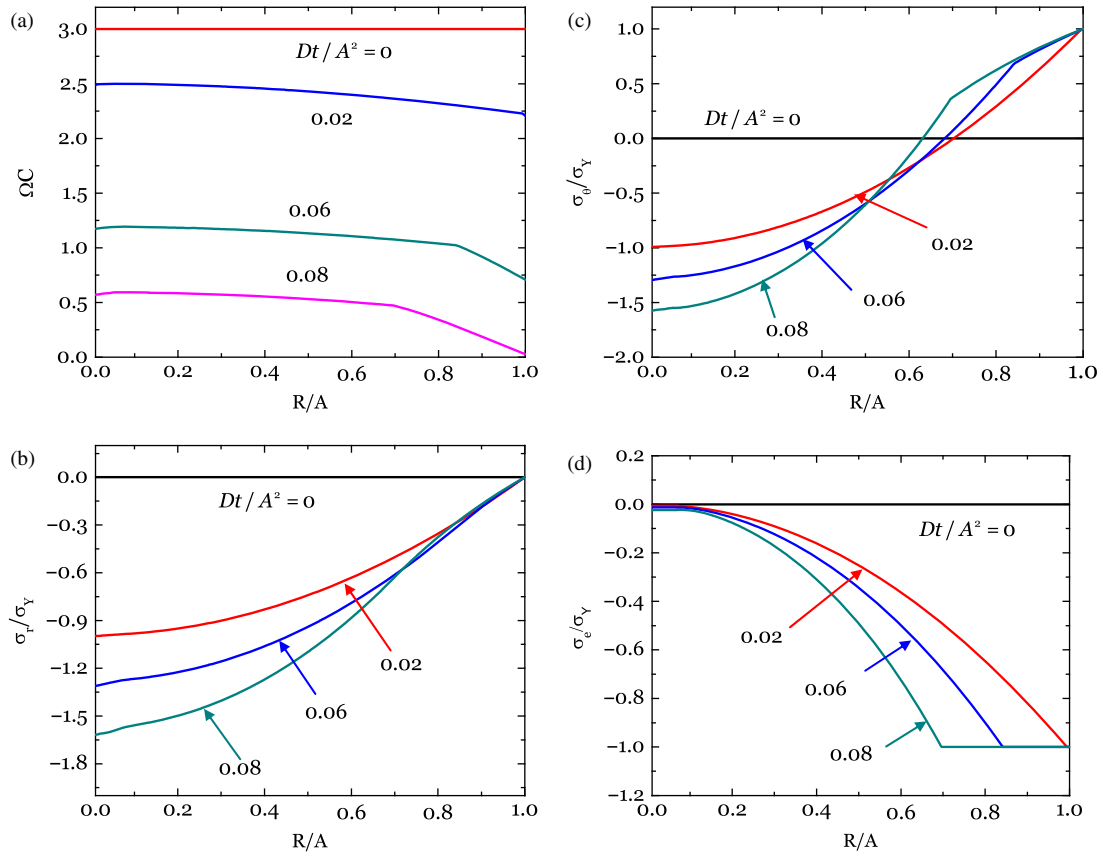

Fig. 9. As a spherical particle is being discharged at the rate of $\tau = 0.5$ h, various fields evolve (a) concentration of lithium, (b) radial stress, (c) hoop stress, and (d) equivalent stress.

A combination of (A-1), (19) and (20) gives that

$$r(R,t) = \left[3\int_0^R (1+\Omega C)R^2 \mathrm{d}R\right]^{1/3} \tag{A-2}$$

Here we have used a condition due to the spherical symmetry of the problem, $r(0, t) = 0$.

The kinetic model (25) can be written in terms of the nominal quantities:

$$J = -\frac{CD}{kT\lambda_r^2}\frac{\partial \mu(R,t)}{\partial R} \tag{A-3}$$

A combination of (A-3) and (24) gives

$$J = -\frac{CD}{(1+\Omega C)^2}\left(\frac{r}{R}\right)^4 \frac{\partial}{\partial R} \times \left[\log\frac{\gamma C}{1+\Omega C} - \frac{\Omega(\sigma_r + 2\sigma_\theta)}{3kT}\right] \tag{A-4}$$

Recall that the flux satisfies the boundary conditions $J(0, t) = 0$ and $J(A, t) = \pm J_0$. The sign of the latter condition depends on whether the particle is being charged or discharged.

The stress $(\sigma_\theta - \sigma_r)$ and the plastic stretch evolve according to the ideal elastic–plastic model, Fig. 3(b). When $|\sigma_r - \sigma_\theta| < \sigma_Y$, the plastic stretch λ_r^p remains fixed, and the elastic stretch is given by $\log \lambda_r^e = (\sigma_r - \sigma_\theta)/E$, which is written as

$$\sigma_r - \sigma_\theta = E\log(\Lambda^{-1/3}\lambda_r/\lambda_r^p) \tag{A-5}$$

when $\sigma_r - \sigma_\theta = \pm\sigma_Y$, the elastic stretch is fixed at $\log \lambda_r^e = \pm\sigma_Y/E$, and the plastic stretch adopts a value

$$\lambda_r^p = \lambda_r \Lambda^{-1/3}\exp\left(\mp\frac{\sigma_Y}{E}\right) \tag{A-6}$$

Integrating (23), we obtain that

$$\sigma_r(R,t) = 2\int_A^R \frac{(\sigma_r - \sigma_\theta)(1+\Omega C)R^2}{r^3}\mathrm{d}R \tag{A-7}$$

Here we have used the boundary condition $\sigma_r(A, t) = 0$.

We use the finite difference method, and divide the interval $0 \le R \le A$ into small elements. The initial condition $C(R, 0)$ is prescribed; for example, we set $C(R, 0) = 0$ to simulate the process of lithiation, and set $C(R, 0) = C_{max}$ to simulate the process of delithiation. The initial values of the function $J(R, 0)$ are set with $J(0, 0) = 0$ and $J(A, 0) = \pm J_0$ at the boundaries, and $J(R, 0) = 0$ at the interior points. We then evolve all functions with a time step Δt. At a given time t, the functions $C(R, t)$ and $J(R, t)$, along with the boundary conditions $J(0, t) = 0$ and $J(A, t) = \pm J_0$, are inserted into (21) to calculate $C(R, t+\Delta t)$. The result is then inserted into (A-2) to calculate $r(R, t+\Delta t)$. The field $\sigma_r(R, t+\Delta t)$ is calculated by the integrating (A-7), where $(\sigma_\theta - \sigma_r)$ is determined by the uniaxial stress–strain relation. We then calculate $J(R, t+\Delta t)$ by using (A-4). This procedure is repeated for the next time step to evolve the fields.

Acknowledgments

Matt Pharr acknowledges the support of the Department of Defense (DoD) through the National Defense Science & Engineering Graduate Fellowship (NDSEG) Program.

This paper is submitted to the *Journal of the American Ceramic Society* for a special issue dedicated to the memory of A. G. Evans.

References

[1]R. A. Huggins, *Advanced Batteries: Materials Science Aspects*. Springer, New York, 2009.

[2]J. Christensen and J. Newman, "Stress Generation and Fracture in Lithium Insertion Materials," *J. Solid State Electrochem.*, **10** [5] 293–319 (2006).

[3]X. C. Zhang, W. Shyy, and A. M. Sastry, "Numerical Simulation of Intercalation-Induced Stress in Li-Ion Battery Electrode Materials," *J. Electrochem. Soc.*, **154** [10] A910–6 (2007).

[4]S. Golmon, K. Maute, S. H. Lee, and M. L. Dunn, "Stress Generation in Silicon Particles During Lithium Insertion," *Appl. Phys. Lett.*, **97** [3] 033111, 3pp (2010).

[5]Y. T. Cheng and M. W. Verbrugge, "Evolution of Stress within a Spherical Insertion Electrode Particle Under Potentiostatic and Galvanostatic Operation," *J. Power Sources*, **190** [2] 453–60 (2009).

[6]Y. H. Hu, X. H. Zhao, and Z. G. Suo, "Averting Cracks Caused by Insertion Reaction in Lithium-Ion Batteries," *J. Mater. Res.*, **25** [6] 1007–10 (2010).

[7]R. A. Huggins and W. D. Nix, "Decrepitation Model for Capacity Loss During Cycling of Alloys in Rechargeable Electrochemical Systems," *Ionics*, **6**, 57–64 (2000).

[8]T. K. Bhandakkar and H. J. Gao, "Cohesive Modeling of Crack Nucleation Under Diffusion Induced Stresses in a Thin Strip: Implications on the Critical Size for Flaw Tolerant Battery Electrodes," *Int. J. Solids Struc.*, **47** [10] 1424–34 (2010).

[9]W. H. Woodford, Y. M. Chiang, and W. C. Carter, "Electrochemical Shock of Intercalation Electrodes: A Fracture Mechanics Analysis," *J. Electrochem. Soc.*, **157** [10] A1052–9 (2010).

[10]K. J. Zhao, M. Pharr, J. J. Vlassak, and Z. G. Suo, "Fracture of Electrodes in Lithium-Ion Batteries Caused by Fast Charging," *J. Appl. Phys.*, **108** [7] 073517, 6pp (2010).

[11]Y. Itou and Y. Ukyo, "Performance of $LiNiCoO_2$ Materials for Advanced Lithium-Ion Batteries," *J. Power Sources*, **146** [1–2] 39–44 (2005).

[12]P. Arora, R. E. White, and M. Doyle, "Capacity Fade Mechanisms and Side Reactions in Lithium-Ion Batteries," *J. Electrochem. Soc.*, **145** [10] 3647–67 (1998).

[13]D. Y. Wang, X. D. Wu, Z. X. Wang, and L. Q. Chen, "Cracking Causing Cyclic Instability of $LiFePO_4$ Cathode Material," *J. Power Sources*, **140** [1] 125–8 (2005).

[14]K. E. Aifantis and J. P. Dempsey, "Stable Crack Growth in Nanostructured Li-Batteries," *J. Power Sources*, **143** [1–2] 203–11 (2005).

[15]L. Y. Beaulieu, K. W. Eberman, R. L. Turner, L. J. Krause, and J. R. Dahn, "Colossal Reversible Volume Changes in Lithium Alloys," *Electrochem. Solid State Lett.*, **4** [9] A137–40 (2001).

[16]W. J. Zhang, "A Review of the Electrochemical Performance of Alloy Anodes for Lithium-Ion Batteries," *J. Power Sources*, **196** [1] 13–24 (2011).

[17]T. Takamura, S. Ohara, M. Uehara, J. Suzuki, and K. Sekine, "A Vacuum Deposited Si Film having a Li Extraction Capacity Over 2000 mAh/g with a Long Cycle Life," *J. Power Sources*, **129** [1] 96–100 (2004).

[18]C. K. Chan, H. L. Peng, G. Liu, K. McIlwrath, X. F. Zhang, R. A. Huggins, and Y. Cui, "High-Performance Lithium Battery Anodes Using Silicon Nanowires," *Nature Nanotechnol.*, **3** [1] 31–5 (2008).

[19]H. Kim, B. Han, J. Choo, and J. Cho, "Three-Dimensional Porous Silicon Particles for Use in High-Performance Lithium Secondary Batteries," *Angew. Chem.-Int. Ed.*, **47** [52] 10151–4 (2008).

[20]V. A. Sethuraman, M. J. Chon, M. Shimshak, V. Srinivasan, and P. R. Guduru, "In situ Measurements of Stress Evolution in Silicon Thin Films During Electrochemical Lithiation and Delithiation," *J. Power Sources*, **195** [15] 5062–6 (2010).

[21]J. W. Choi, J. McDonough, S. Jeong, J. S. Yoo, C. K. Chan, and Y. Cui, "Stepwise Nanopore Evolution in One-Dimensional Nanostructures," *Nano Lett.*, **10** [4] 1409–13 (2010).

[22]V. A. Sethuraman, V. Srinivasan, A. F. Bower, and P. R. Guduru, "In situ Measurements of Stress-Potential Coupling in Lithiated Silicon," *J. Electrochem. Soc.*, **157** [11] A1253–61 (2010).

[23]K. J. Zhao, M. Pharr, J. J. Vlassak, and Z. G. Suo, "Inelastic Hosts as Electrodes for High-Capacity Lithium-Ion Batteries," *J. Appl. Phys.*, **109** [1] 016110, 3pp (2011).

[24]E. H. Lee, "Elastic–Plastic Deformation at Finite Strains," *J. Appl. Mech.*, **36** [1] 1–8 (1969).

[25]M. N. Silberstein and M. C. Boyce, "Constitutive Modeling of the Rate, Temperature, and Hydration Dependent Deformation Response of Nafion to Monotonic and Cyclic Loading," *J. Power Sources*, **195** [17] 5692–706 (2010).

[26]M. Ben Amar and A. Goriely, "Growth and Instability in Elastic Tissues," *J. Mech. Phys. Solids*, **53** [10] 2284–319 (2005).

[27]T. Song, J. L. Xia, J. H. Lee, D. H. Lee, M. S. Kwon, J. M. Choi, J. Wu, S. K. Doo, H. Chang, W. Il Park, D. S. Zang, H. Kim, Y. G. Huang, K. C. Hwang, J. A. Rogers, and U. Paik, "Arrays of Sealed Silicon Nanotubes as Anodes for Lithium Ion Batteries," *Nano Lett.*, **10** [5] 1710–6 (2010).

[28]R. Hill, *The Mathematical Theory of Plasticity*. Oxford University Press, Oxford, 1950.

[29]N. Ding, J. Xu, Y. X. Yao, G. Wegner, X. Fang, C. H. Chen, and I. Lieberwirth, "Determination of the Diffusion Coefficient of Lithium Ions in Nano-Si," *Solid State Ionics*, **180** [2–3] 222–5 (2009). □